Vibration Analysis of Carotid Arteries Conveying Non-Newtonian Blood Flow Surrounding by Tissues

A.H. Ghorbanpour Arani [1], A. Rastgoo [1], A. Ghorbanpour Arani [2, 3] *, R. Kolahchi [2]

[1]*Faculty of Mechanical Engineering, University of Tehran, Tehran, Iran*
[2]*Faculty of Mechanical Engineering, University of Kashan, Kashan, Iran*
[3]*Institute of Nanoscience & Nanotechnology, University of Kashan, Kashan, Iran*

ABSTRACT

The high blood rate that often occurs in arteries may play a role in artery failure and tortuosity which leads to blackouts, transitory ischemic attacks and other diseases. However, vibration and instability analysis of carotid arteries are lacking. The objective of this study is to investigate the vibration and instability of the carotid arteries conveying blood under axial tension with surrounding tissue support. Arteries are modeled as elastic cylindrical vessels based on first order shear deformation theory (FSDT) within an elastic substrate. The elastic medium is simulated with visco-Pasternak foundation. The blood flow in carotid artery is modeled with non-Newtonian fluid based on Carreau, power law and Casson models. Applying energy method, Hamilton principle and differential quadrature method (DQM), the frequency, critical blood velocity and transverse displacement of the carotid arteries are obtained. It can be seen that increasing the tissue stiffness would delay critical blood velocity. The current model provides a powerful tool for further experimental investigation arteries tortuosity. In addition, the dimensionless transverse displacement predicted by Newtonian model is lower than that of non-Newtonian models.

© 2016 IAU, Arak Branch.All rights reserved.

Keywords : Carotid artery; Non-Newtonian fluid; Critical blood velocity; FSDT; Tissue matrix.

1 INTRODUCTION

BIOMECHANICAL systems such as arteries conveying blood may be affected by vibration and instability which may lead to serious or even fatal situations such as disturbances in blood flow prevent blood flow to distal organs, atherosclerosis, failure and tortuosity. Blackouts, transitory ischemic attacks, stroke, vertigo, syncopes, persistent tinnitus, hinder proper vascular and tissue regeneration [1-6] are some of the symptoms which result from mentioned serious or fatal situations. Hence, it is important to present a biomechanical model for vibration and instability analysis of arteries conveying blood.

Despite the clinical importance of vibration and buckling in the arteries, few researchers worked in this area. Jackson et al. [7] investigated arterial tortuosity induced by longitudinal tension. They concluded experimentally that the tortuosity may be due to the mechanical buckling of the arteries. For the first time, Han [8-12] presented a biomechanical model for the artery buckling. The stability of arteries under blood pressure was studied by Han [8] to determine the critical buckling loads. He found that arteries may buckle and become tortuous due to reduced axial

---

*Corresponding author. Tel.: +98 31 55912450; Fax: +98 31 55912424.
E-mail address: aghorban@kashanu.ac.ir (A.Ghorbanpour Arani).

strain, hypertensive pressure and a weakened wall. In another work, the arterial buckling equation using a nonlinear elastic thick-walled cylindrical model with residual stress was developed by Han [9]. One of the important results of this study was improving the stability of the arteries by increasing the buckling pressure especially in the high stretch ratio range. Furthermore, Han [10] analyzed the buckling of blood vessels under lumen pressure with surrounding tissue support. He concluded that blood vessels do take higher order mode shapes when buckling inside an elastic substrate while they take the basal mode shape without the substrate. The artery critical buckling pressure under pulsatile pressure both experimentally and theoretically was determined by Liu and Han [11] based on beam-column model. In another work by the same authors [12], arteriole critical buckling pressure and buckling pattern during arteriole remodeling were investigated. They shown that arteriole buckling mode number increased with increasing axial growth ratio, but decreased with increasing radius growth ratio and wall thickness.

With respect to developmental works on biomechanical analysis of arteries, it should be noted that none of the research mentioned above, have considered blood flow in the arteries. In the simulation of blood flow in arteries, it is important to consider the nature of blood as a fluid. It is well known that blood behaves as a non-Newtonian fluid, particularly at low shear rates [13]. Cho and Kensey [14] investigated effects of the non-Newtonian viscosity of blood flows in a diseased arterial vessel considering steady blood flow. The steady flow of Newtonian fluid through a catheterized curved artery with stenosis was studied by Dash et al. [15]. The non-Newtonian fluid flow in a bifurcation model with a non-planar daughter branch was investigated by Chen and Lu [16] using finite element method to solve the three-dimensional Navier–Stokes equations coupled with a non-Newtonian constitutive model, in which the shear thinning behavior of the blood fluid was incorporated by the Carreau–Yasuda model. Johnston et al. [17] used five non-Newtonian blood models, as well as the usual Newtonian model of blood viscosity to study the wall shear stress in arteries. Mandal [18] solved numerically the problem of non-Newtonian and nonlinear blood flow through a stenosed artery where the non-Newtonian rheology of the flowing blood is characterized by the generalized Power-law model. The effects of catheterization and non-Newtonian nature of blood in small arteries on velocity, flow resistance and wall shear stress were analyzed mathematically by Sankar and Hemalatha [19] considering blood as a Herschel–Bulkley fluid and assuming the steady flow. Boyd et al. [20] analyzed of the Casson and Carreau-Yasuda non-Newtonian blood models in steady and oscillatory flows using the lattice Boltzmann method.

Whereas to the authors' knowledge, not any research has been found yet on the vibration and instability analysis of carotid arteries conveying non-Newtonian blood surrounding by tissues. However, for the first time, the carotid arteries are modeled as elastic circular cylinders based on FSDT and the surrounding tissues are modeled as visco elastic matrix. The objectives of this study are to establish a model of blood flow in carotid arteries vibration inside an elastic substrate and thus to determine the frequency and critical blood velocity of the arteries. Furthermore, the effects of surrounding tissue support and non-Newtonian fluid models on the critical blood velocity, frequency pattern and transverse displacement of carotid arteries are considered.

2   A BIOMECHANICAL MODEL FOR CAROTID ARTERIES

2.1 Stress-strain relation

An image of arteries embedded in tissues of human body is shown in Fig. 1(a). A biomechanical model of an artery with density of ρ_A conveying pulsating blood is depicted in Fig. 1(b) in which geometrical parameters of length L, radius R and thickness h are indicated. The cylindrical polar coordinates (r,θ,x), where r,θ and x denote the radial, circumferential and axial coordinates, respectively, is used. The artery is surrounded by tissue which is simulated by visco-Pasternak foundation.
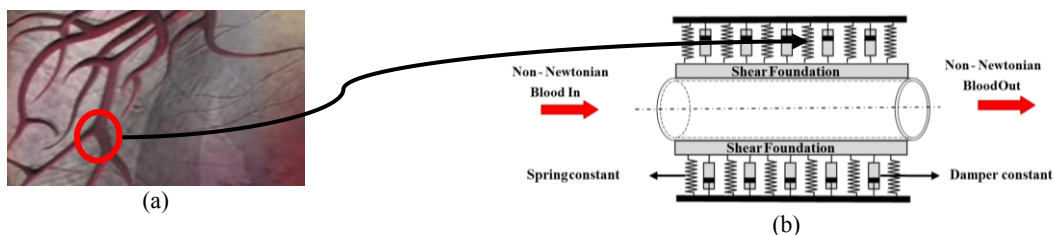

Fig.1
(a) Arteries in tissues of human body (b) A biomechanical model for arteries surrounded by tissues conveying blood.

Generally, stress-strain relation for isotropic material in polar coordinate can be written as:

$$
\begin{Bmatrix} \sigma_{xx} \\ \sigma_{\theta\theta} \\ \sigma_{zz} \\ \sigma_{\theta z} \\ \sigma_{zx} \\ \sigma_{x\theta} \end{Bmatrix} = \begin{bmatrix} C_{11} & C_{12} & C_{13} & 0 & 0 & 0 \\ C_{12} & C_{22} & C_{23} & 0 & 0 & 0 \\ C_{13} & C_{23} & C_{33} & 0 & 0 & 0 \\ 0 & 0 & 0 & C_{44} & 0 & 0 \\ 0 & 0 & 0 & 0 & C_{55} & 0 \\ 0 & 0 & 0 & 0 & 0 & C_{66} \end{bmatrix} \times \begin{Bmatrix} \varepsilon_{xx} \\ \varepsilon_{\theta\theta} \\ \varepsilon_{zz} \\ 2\varepsilon_{\theta z} \\ 2\varepsilon_{zx} \\ 2\varepsilon_{x\theta} \end{Bmatrix},
\tag{1}
$$

where C_{ij} are elastic constant. At real life, arteries properties depend on the time variation. This model represents, as the stress is released, the material gradually relaxes to its undeformed state. By considering this model, C_{ij} are as follows

$$
C_{ij} = C_{ij}\left(1 + g\frac{\partial}{\partial t}\right),
\tag{2}
$$

where g is viscoelastic coefficient. Based on MCST, the displacement components of an arbitrary point in the cylindrical shell in terms of x, θ and z coordinates, denoted by $\tilde{u}, \tilde{v}$ and $\tilde{w}$ can be written as [21, 22]:

$$
\begin{aligned}
\tilde{u}(x,\theta,z,t) &= u(x,\theta,t) + z\,\phi_x(x,\theta,t), \\
\tilde{v}(x,\theta,z,t) &= v(x,\theta,t) + z\,\phi_\theta(x,\theta,t), \\
\tilde{w}(x,\theta,z,t) &= w(x,\theta,t),
\end{aligned}
\tag{3}
$$

where *u,v* and *w* are displacement components of the mid-plane in the axial, circumferential and radial directions, respectively, ϕ_x and ϕ_θ are the rotations of a transverse normal about the axial and circumferential directions. The strain-displacement relations are given by:

$$
\varepsilon_{xx} = \frac{\partial u}{\partial x} + \frac{1}{2}\left(\frac{\partial w}{\partial x}\right)^2 + z\frac{\partial \phi_x}{\partial x},
\tag{4a}
$$

$$
\varepsilon_{\theta\theta} = \frac{1}{R}\left(w + \frac{\partial v}{\partial \theta}\right) + \frac{1}{2R^2}\left(\frac{\partial w}{\partial \theta}\right)^2 + \frac{z}{R}\frac{\partial \phi_\theta}{\partial \theta},
\tag{4b}
$$

$$
\gamma_{x\theta} = \frac{\partial v}{\partial x} + \frac{1}{R}\left(\frac{\partial u}{\partial \theta} + \frac{\partial w}{\partial \theta}\frac{\partial w}{\partial x}\right) + z\left(\frac{\partial \phi_\theta}{\partial x} + \frac{1}{R}\frac{\partial \phi_x}{\partial \theta}\right),
\tag{4c}
$$

$$
\gamma_{xz} = \phi_x + \frac{\partial w}{\partial x},
\tag{4d}
$$

$$
\gamma_{z\theta} = \frac{1}{R}\left(\frac{\partial w}{\partial \theta} - v - z\,\phi_\theta\right) + \phi_\theta.
\tag{4e}
$$

2.2. Motion equations

To derive the equations of motion of visco-arteries surrounding by visco-tissues, the Hamilton's principle is utilized, which is defined as follows [22]:

$$\int_0^T \left(\delta U - \delta K - \delta W_{Blood} - \delta W_{tissue} \right) dt = 0, \tag{5}$$

where U is the potential energy, K is the kinetic energy, W_{tissue} and W_{Blood} are the works done by tissue and non-newtonian pulsating blood flow, respectively.

2.2.1 Potential energy

The potential energy of the artery can be written as follows

$$U = \frac{1}{2} \iiint_V \left(\sigma_{xx} \varepsilon_{xx} + \sigma_{\theta\theta} \varepsilon_{\theta\theta} + \sigma_{x\theta} \gamma_{x\theta} + \sigma_{xz} \gamma_{xz} + \sigma_{z\theta} \gamma_{z\theta} \right) dV, \tag{6}$$

Substituting Eqs. (1)-(4) into Eq. (6) yields

$$U = \int_0^{2\pi} \int_0^L \left[N_{xx} \left(\frac{\partial u}{\partial x} \right) + N_{\theta\theta} \left(\frac{w}{R} + \frac{1}{R} \frac{\partial v}{\partial \theta} \right) + N_{x\theta} \left(\frac{\partial v}{\partial x} + \frac{1}{R} \frac{\partial u}{\partial \theta} \right) + M_{xx} \frac{\partial \phi_x}{\partial x} + \frac{M_{\theta\theta}}{R} \frac{\partial \phi_\theta}{\partial \theta} \right.$$
$$\left. + M_{x\theta} \frac{\partial \phi_\theta}{\partial x} + \frac{M_{x\theta}}{R} \frac{\partial \phi_\theta}{\partial \theta} + Q_x \left(\phi_x + \frac{\partial w}{\partial x} \right) + Q_\theta \left(\frac{1}{R} \frac{\partial w}{\partial \theta} - \frac{v}{R} + \phi_x \right) \right\} R dx d\theta. \tag{7}$$

The resultant forces $\left(N_{xx}, N_{\theta\theta}, N_{x\theta} \right)$, moment resultants $\left(M_{xx}, M_{\theta\theta}, M_{x\theta} \right)$ and transverse shear force resultants $\left(Q_x, Q_\theta \right)$ are defined as:

$$\begin{Bmatrix} N_{xx} \\ N_{\theta\theta} \\ N_{x\theta} \end{Bmatrix} = \int_{-h/2}^{h/2} \begin{Bmatrix} \sigma_{xx} \\ \sigma_{\theta\theta} \\ \sigma_{x\theta} \end{Bmatrix} dz, \quad \begin{Bmatrix} M_{xx} \\ M_{\theta\theta} \\ M_{x\theta} \end{Bmatrix} = \int_{-h/2}^{h/2} \begin{Bmatrix} \sigma_{xx} \\ \sigma_{\theta\theta} \\ \sigma_{x\theta} \end{Bmatrix} z dz, \quad \begin{Bmatrix} Q_x \\ Q_\theta \end{Bmatrix} = k \int_{-h/2}^{h/2} \begin{Bmatrix} \sigma_{xz} \\ \sigma_{z\theta} \end{Bmatrix} dz, \tag{8}$$

where k is shear correction factor.

2.2.2 Kinetic energy

The kinetic energy of the artery can be expressed as:

$$U = \frac{\rho_A}{2} \iiint_V \left[\left(\frac{\partial \tilde{u}}{\partial t} \right)^2 + \left(\frac{\partial \tilde{v}}{\partial t} \right)^2 + \left(\frac{\partial \tilde{w}}{\partial t} \right)^2 \right] dV, \tag{9}$$

2.2.3 Tissues work

As reported by the researchers, the effect of surrounding tissue is very important for biomechanical analysis of arteries [10]. In previous works, the tissues effects are simulated by spring constants only [10,12]. In this study, in order to realistic simulation of the tissues and muscles with elastic matrix, the visco-Pasternak foundation is considered including the spring constants (k_w), shear layer (k_g) and damping coefficients (C_d) which can be expressed as [23, 24]

$$W_{tissue} = \int_0^{2\pi} \int_0^L \left(-k_w w + k_g \nabla^2 w - C_d \dot{w} \right) w dA, \tag{10}$$

2.2.4 Non- Newtonian blood flow work

Consider the flow of blood in an artery in which the flow is assumed to be axially symmetric, laminar, steady and fully developed. The basic momentum governing equation of the flow simplifies to

$$\rho_b \frac{\partial v_r}{\partial t} = -\frac{\partial P}{\partial r} + \frac{1}{r}\frac{\partial \tau_{r\theta}}{\partial \theta} - \frac{\tau_{\theta\theta}}{r} + \frac{\partial \tau_{xr}}{\partial x},$$
(11)

where ρ_b and P are blood mass density and flow blood pressure, respectively. The blood force acted on the artery can be calculated from Eq. (11). Since the velocity and acceleration of the artery and blood at the point of contact between them are equal [25], we have

$$v_r = \frac{dw}{dt},$$
(12)

where

$$\frac{d}{dt} = \frac{\partial}{\partial t} + v_x \frac{\partial}{\partial x},$$
(13)

The case of pulsating blood flow is assumed harmonically fluctuating, as follows

$$V_c = V_0(1 + \alpha \cos(\omega t)),$$
(14)

where V_0 is the mean flow velocity, α is the amplitude of the harmonic fluctuation (assumed small) and ω its pulsation frequency of heart.

In Eq. (11), shear stress (τ) is dependent to viscosity μ which can be expressed as follows:

$$\tau_{r\theta} = \mu \frac{1}{r}\frac{\partial v_r}{\partial \theta},$$
(15)

$$\tau_{\theta\theta} = 2\mu \frac{v_r}{r},$$
(16)

$$\tau_{rx} = \mu \frac{\partial v_r}{\partial x},$$
(17)

For a non-Newtonian fluid, μ is a function of shear rate ($\dot{\gamma}$), while for a Newtonian fluid μ is a constant and independent of the $\dot{\gamma}$. Herein, a Newtonian model and three models for non- Newtonian blood are considered as: [17]

Newtonian model

$$\mu = 0.0345 \ P$$
(18)

Carreau model

$$\mu = \mu_\infty + (\mu_0 - \mu_\infty)\left[1 + (\lambda\dot{\gamma})^2\right]^{(n-1)/2}$$
(19)

where $\lambda = 3.313 s, n = 0.3568, \mu_0 = 0.56 \ P$ and $\mu_\infty = 0.0345$ P.

Power Law

$$\mu = \mu_0 (\dot{\gamma})^{n-1} \tag{20}$$

where $n = 0.6$ and $\mu_0 = 0.035$ P.

Casson model

$$\mu = \left[(\eta^2 J_2)^{1/4} + 2^{-0.5} \tau_y^{0.5} \right] J_2^{-0.5} \tag{21}$$

where $|\dot{\gamma}| = 2\sqrt{J_2}$, $\tau_y = 0.1(0.625H)^3$ and $\eta = \eta_0 (1-H)^{-2.5}$ with $\eta_0 = 0.012$ P and $H = 0.37$.

Finally, using Eqs. (12)-(17) and combination with Eq. (11), the pulsating non-Newtonian blood flow work may be written as:

$$W_{Blood} = \int F_{Blood} \, w dA = \int \left[-\rho_b h_b \left(\frac{\partial^2 w}{\partial t^2} + 2v_x \frac{\partial^2 w}{\partial x \partial t} + v_x^2 \frac{\partial^2 w}{\partial x^2} \right) + \frac{h_b}{R^2} \frac{\partial}{\partial \theta} \left(\mu(\dot{\gamma}) \left(\frac{\partial^2 w}{\partial \theta \partial t} + v_x \frac{\partial^2 w}{\partial \theta \partial x} \right) \right) \right.$$
$$\left. - \frac{2h_b}{R} \left(\mu(\dot{\gamma}) \left(\frac{\partial w}{\partial t} + v_x \frac{\partial w}{\partial x} \right) \right) + h_b \frac{\partial}{\partial x} \left(\mu(\dot{\gamma}) \left(\frac{\partial^2 w}{\partial x \partial t} + v_x \frac{\partial^2 w}{\partial x^2} \right) \right) \right] w dA, \tag{22}$$

According to Hamilton's principal (i.e. Eq. (5)), the motion equations are obtained as follows:

$$A_{11} \left(\frac{\partial^2 u}{\partial x^2} + g \frac{\partial^3 u}{\partial x^2 \partial t} \right) + \frac{A_{12}}{R} \left(\frac{\partial w}{\partial x} + \frac{\partial^2 v}{\partial x \partial \theta} + g \frac{\partial^2 w}{\partial t \partial x} + g \frac{\partial^3 v}{\partial x \partial \theta \partial t} \right)$$
$$+ \frac{A_{66}}{R} \left(\frac{1}{R} \frac{\partial^2 u}{\partial \theta^2} + \frac{\partial^2 v}{\partial x \partial \theta} + \frac{g}{R} \frac{\partial^3 u}{\partial \theta^2 \partial t} + g \frac{\partial^3 v}{\partial x \partial \theta \partial t} \right) = \rho_A h \frac{\partial^2 u}{\partial t^2}, \tag{23}$$

$$A_{66} \left(\frac{\partial^2 v}{\partial x^2} + \frac{1}{R} \frac{\partial^2 u}{\partial x \partial \theta} + g \frac{\partial^3 v}{\partial x^2 \partial t} + \frac{g}{R} \frac{\partial^3 u}{\partial x \partial \theta \partial t} \right) + \frac{A_{12}}{R} \left(\frac{\partial^2 u}{\partial x \partial \theta} + g \frac{\partial^3 u}{\partial t \partial x \partial \theta} \right) + \frac{A_{22}}{R^2} \left(\frac{\partial w}{\partial \theta} + \frac{\partial^2 v}{\partial \theta^2} \right.$$
$$\left. + g \frac{\partial^2 w}{\partial t \partial \theta} + g \frac{\partial^3 v}{\partial t \partial \theta^2} \right) + \frac{kA_{44}}{R} \left(\frac{1}{R} \frac{\partial w}{\partial \theta} - \frac{v}{R} + \phi_\theta + \frac{g}{R} \frac{\partial^2 w}{\partial t \partial \theta} - \frac{g}{R} \frac{\partial v}{\partial t} + g \frac{\partial \phi_\theta}{\partial t} \right) = \rho_A h \frac{\partial^2 v}{\partial t^2}, \tag{24}$$

$$kA_{55} \left(\frac{\partial w^2}{\partial x^2} + \frac{\partial \phi_x}{\partial x} + g \frac{\partial^3 w}{\partial x^2 \partial t} + g \frac{\partial^2 \phi_x}{\partial x \partial t} \right) + \frac{kA_{44}}{R} \left(\frac{1}{R} \frac{\partial w^2}{\partial \theta^2} - \frac{1}{R} \frac{\partial v}{\partial \theta} + \frac{\partial \phi_\theta}{\partial \theta} + \frac{g}{R} \frac{\partial^3 w}{\partial \theta^2 \partial t} - \frac{g}{R} \frac{\partial^2 v}{\partial \theta \partial t} + g \frac{\partial^2 \phi_\theta}{\partial \theta \partial t} \right)$$
$$- \frac{A_{12}}{R} \left(\frac{\partial u}{\partial x} + g \frac{\partial^2 u}{\partial t \partial x} \right) + \frac{A_{22}}{R^2} \left(w + \frac{\partial v}{\partial \theta} + g \frac{\partial w}{\partial t} + g \frac{\partial^2 v}{\partial t \partial \theta} \right) + \frac{\partial}{\partial x} \left(N_{xx}^M \frac{\partial w}{\partial x} \right) + \frac{1}{R^2} \frac{\partial}{\partial \theta} \left(N_{\theta\theta}^M \frac{\partial w}{\partial \theta} \right)$$
$$+ \frac{1}{R} \frac{\partial}{\partial \theta} \left(N_{x\theta}^M \frac{\partial w}{\partial x} \right) + \frac{1}{R} \frac{\partial}{\partial x} \left(N_{x\theta}^M \frac{\partial w}{\partial \theta} \right) - k_w w + k_g \nabla^2 w - C_d \dot{w} - \rho_b h_b \left(\frac{\partial^2 w}{\partial t^2} + 2v_x \frac{\partial^2 w}{\partial x \partial t} + v_x^2 \frac{\partial^2 w}{\partial x^2} \right)$$
$$+ \frac{h_b}{R^2} \frac{\partial}{\partial \theta} \left(\mu(\dot{\gamma}) \left(\frac{\partial^2 w}{\partial \theta \partial t} + v_x \frac{\partial^2 w}{\partial \theta \partial x} \right) \right) \left(\mu(\dot{\gamma}) \left(\frac{\partial w}{\partial t} + v_x \frac{\partial w}{\partial x} \right) \right) + h_b \frac{\partial}{\partial x} \left(\mu(\dot{\gamma}) \left(\frac{\partial^2 w}{\partial x \partial t} + v_x \frac{\partial^2 w}{\partial x^2} \right) \right) - \frac{2h_b}{R} = \rho_A h \frac{\partial^2 w}{\partial t^2}, \tag{25}$$

$$D_{11} \left(\frac{\partial^2 \phi_x}{\partial x^2} + g \frac{\partial^3 \phi_x}{\partial x^2 \partial t} \right) + \frac{D_{12}}{R} \left(\frac{\partial^2 \phi_\theta}{\partial x \partial \theta} + g \frac{\partial^2 \phi_\theta}{\partial x \partial \theta \partial t} \right) + \frac{D_{66}}{R} \left(\frac{1}{R} \frac{\partial^2 \phi_x}{\partial \theta^2} + \frac{\partial^2 \phi_\theta}{\partial x \partial \theta} \right.$$
$$\left. + \frac{g}{R} \frac{\partial^3 \phi_x}{\partial \theta^2 \partial t} + g \frac{\partial^3 \phi_\theta}{\partial x \partial \theta \partial t} \right) - kA_{55} \left(\frac{\partial w}{\partial x} + \phi_x + g \frac{\partial^w w}{\partial x \partial t} + g \frac{\partial \phi_x}{\partial t} \right) = -\frac{1}{12} \rho_A h^3 \frac{\partial^2 \phi_x}{\partial t^2}, \tag{26}$$

$$\frac{D_{12}}{R}\left(\frac{\partial^2 \phi_x}{\partial x \partial \theta} + g \frac{\partial^3 \phi_x}{\partial x \partial \theta \partial t}\right) + D_{22}\left(\frac{\partial^2 \phi_\theta}{\partial x^2} + g \frac{\partial^2 \phi_\theta}{\partial x^2 \partial t}\right) + \frac{D_{66}}{R}\left(\frac{1}{R}\frac{\partial^2 \phi_\theta}{\partial x^2} + \frac{\partial^2 \phi_x}{\partial x \partial \theta}\right)$$

$$+ \frac{g}{R}\frac{\partial^3 \phi_\theta}{\partial x^2 \partial t} + g \frac{\partial^3 \phi_x}{\partial x \partial \theta \partial t}\right) - kA_{55}\left(\frac{\partial w}{\partial \theta} + \phi_\theta + g \frac{\partial w}{\partial \theta \partial t} + g \frac{\partial \phi_\theta}{\partial t}\right) = -\frac{1}{12}\rho_A h^3 \frac{\partial^2 \phi_x}{\partial t^2}, \tag{27}$$

where A_{ij}, D_{ij} $(i, j = 1, 2, ..., 6)$ may be expressed as:

$$A_{ij} = \int_{-h/2}^{h/2} C_{ij} dz, \quad D_{ij} = \int_{-h/2}^{h/2} C_{ij} z^2 dz, \tag{28}$$

Also, in Eq. (25), $N_{\theta\theta}{}^M = N_{x\theta}{}^M = 0$ and $N_{xx}{}^M$ represents the axial (longitudinal) tension N (i.e. $N_{xx}^M = -N$) [10].

2.4 Solution procedure

The method used in this study is DQM. In this method, the partial derivatives of a function (F) are approximated by a specific variable, at discontinuous points in domain as a set of weighting series and its amount presented by the function itself at that point and other points throughout the domain. Let F be a function representing u, v, w, ϕ_x and ϕ_θ with respect to variables x and θ in the following domain of ($0 < x < L, 0 < \theta < 2\pi$) having $N_x \times N_\theta$ grid points along these variables. The nth-order partial derivative of $F(x, \theta)$ with respect to x, the mth-order partial derivative of $F(x, \theta)$ with respect to θ and the $(n + m)^{th}$-order partial derivative of $F(x, \theta)$ with respect to both x and θ may be expressed discretely [26, 27] at the point (x_i, θ_i) as:

$$\frac{d^n F(x_i, \theta_j)}{dx^n} = \sum_{k=1}^{N_x} A_{ik}^{(n)} F(x_k, \theta_j) \qquad n = 1, ..., N_x - 1, \tag{29}$$

$$\frac{d^m F(x_i, \theta_j)}{d\theta^m} = \sum_{l=1}^{N_\theta} B_{jl}^{(m)} F(x_i, \theta_l) \qquad m = 1, ..., N_\theta - 1, \tag{30}$$

$$\frac{d^{n+m} F(x_i, \theta_j)}{dx^n d\theta^m} = \sum_{k=1}^{N_x} \sum_{l=1}^{N_\theta} A_{ik}^{(n)} B_{jl}^{(m)} F(x_k, \theta_l), \tag{31}$$

where $A_{ik}^{(n)}$ and $B_{jl}^{(m)}$ are the weighting coefficients associated with n^{th}-order partial derivative of $F(x, \theta)$ with respect to x at the discrete point x_i and m^{th}-order derivative with respect to θ at θ_i, respectively, whose recursive formulae can be found in [26, 27]. A more superior choice for the positions of the grid points is Chebyshev polynomials as expressed in [26, 27]. According to DQM, mechanical simply supported boundary conditions at both ends of the artery may be written as:

$$\begin{cases} w_{i1} = v_{i1} = u_{i1} = 0, & \sum_{j=1}^{N_\theta} A_{2j}^{(2)} w_{ji} = 0 \\ \\ w_{N_x i} = v_{N_x i} = u_{N_x i} = 0, & \sum_{j=1}^{N_\theta} A_{(N_x-1)j}^{(2)} w_{ji} = 0 \end{cases} \qquad for \quad i = 1...N_\theta. \tag{32}$$

Applying DQM to Eqs. (23)-(27) and combining with above equation, the governing equations can be expressed in matrix form as:

$$\left[\begin{bmatrix} K_{bb} \end{bmatrix} \begin{bmatrix} K_{bd} \end{bmatrix} \\ \begin{bmatrix} K_{db} \end{bmatrix} \begin{bmatrix} K_{dd} \end{bmatrix}\right]\left\{\begin{Bmatrix} Y_b \end{Bmatrix} \\ \begin{Bmatrix} Y_d \end{Bmatrix}\right\} + \left[\begin{bmatrix} 0 \end{bmatrix} \begin{bmatrix} 0 \end{bmatrix} \\ \begin{bmatrix} C_{db} \end{bmatrix} \begin{bmatrix} C_{dd} \end{bmatrix}\right]\left\{\begin{Bmatrix} \dot{Y}_b \end{Bmatrix} \\ \begin{Bmatrix} \dot{Y}_d \end{Bmatrix}\right\} + \left[\begin{bmatrix} 0 \end{bmatrix} \begin{bmatrix} 0 \end{bmatrix} \\ \begin{bmatrix} M_{db} \end{bmatrix} \begin{bmatrix} M_{dd} \end{bmatrix}\right]\left\{\begin{Bmatrix} \ddot{Y}_b \end{Bmatrix} \\ \begin{Bmatrix} \ddot{Y}_d \end{Bmatrix}\right\} = 0, \tag{33}$$

where Y is the displacement vector, $[M]$ is the mass matrix, $[C]$ is the damping matrix and $[K]$ is the stiffness matrix. Furthermore, the indexes of b and d represent boundary and domain points, respectively. Assuming $\{\{Y_b\},\{Y_d\}\} = \{\bar{y}_b, \bar{y}_d\}e^{\lambda t}$ yields the following standard eigenvalue problem

$$AZ = \lambda Z, \qquad Z = \{\{Y_b\},\{\dot{Y}_b\}\}^T, \tag{34}$$

where λ is the eigenvalue and matrix A can be defined as:

$$A = \begin{bmatrix} 0 & I \\ -M^{-1}K & -M^{-1}C \end{bmatrix}, \tag{35}$$

where $[0]$ and $[I]$ are the zero and unitary matrices, respectively. Using Eq. (35) in conjunction with a direct iterative method, the frequency of the artery may be obtained.

3   NUMERICAL RESULTS

Numerical results are presented in this section for carotid arteries conveying non-Newtonian blood surrounding by living cells based on known DQM. For illustration purpose, an artery with length, $L = 45\ mm$, outer radius, $R_2 = 5.38\ mm$, inner radius, $R_1 = 3.38\ mm$, thickness, $h = 1\ mm$ and Young modulus of 200 KPa is considered [11].

   Generally, in all of the figures, the frequency of artery decrease as blood velocity increases which physically implies that the artery is stable. For zero frequency, the artery becomes unstable and the corresponding blood velocity is called the critical blood velocity. Therefore, with increasing blood velocity, arteries stability decreases and becomes susceptible to buckling. It should be noted that the range of blood velocity is selected in this part according to the literature in this field [28].

   Fig. 2 illustrates the frequency of the artery versus blood velocity for Newtonian and three cases of non-Newtonian flow fluids for blood flow. One of the main advantages of this study is considering the non-Newtonian nature of the blood flow using Carreau, Casson and power law models. It can be evidently seen that the critical blood velocity predicted by Newtonian model is higher than that of non-Newtonian models. Because of the shear-thinning behavior of the non-Newtonian fluid, the shear force acting on the arteries increases which leads to lower critical blood velocity and frequency of the arteries. In addition, the critical blood velocity and frequency obtained from Carreau fluid is lower than that of Casson fluid and higher than that of power law fluid. It should be noted that using from the aforementioned non-Newtonian fluid models is related to value of the strain which is obtained experimentally and computationally by the researchers [28, 29].
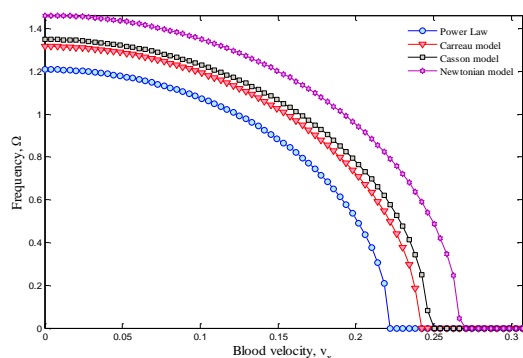

Fig.2
Frequency of arteries versus blood velocity for Newtonian and non-Newtonian blood flow models.

Presented in Figs. 3 and 4 are the effect of the surrounding tissue matrix on the frequency and instability of the arteries as a function of blood velocity. Fig. 3 is given to highlight the spring constant of the elastic matrix without k_g and C_d. Noted that the spring constant stiffness of the tissue is selected the same as [10] in the range of $0 < k_w < 40\ KPa$. As can be seen, with increasing the tissue stiffness, critical blood velocity increases. On the other hand, instability of the artery will occur at higher blood velocities as the tissue becomes stronger and contiguous. Hence, reinforce of the tissue with different ways such as sport prevent from artery failure and tortuosity which leads to symptoms such as blackouts, transitory ischemic attacks, hypertension, diabetes, aging, atherosclerosis and other vascular diseases [10]. These results are the same as those presented by other researchers [10, 12] and clinical reports [30] which contiguous tissue and muscles lead to wound recovery and improve the arteries and vein graft stability.

From the above discussion, it can be concluded that the effect of surrounding tissue is very important for studying the biomechanical basis for arteries vibration and instability. However, in order to realistic simulation of the tissues with elastic matrix, the visco-Pasternak foundation is considered here. The effects of elastic matrix type on the vibration and instability of the arteries are demonstrated in Fig. 4 for five below cases:

Case 1: Vibration and instability of the arteries without surrounding tissue effects (i.e. without elastic matrix).

Case 2: Simulating of the surrounding tissue with spring constants only (i.e. Winkler medium). Noted that this medium is applied in Fig. 3.

Case 3: Simulating of the surrounding tissue with spring constants and damping coefficients (i.e. visco-Winkler medium).

Case 4: Simulating of the surrounding tissue with spring constants and shear layer (i.e. Pasternak medium).

Case 5: Simulating of the surrounding tissue with spring constants, shear layer and damping coefficients (i.e. visco-Pasternak medium).

It is observed from Fig. 4 that the critical blood velocity and frequency obtained from visco-Winkler and visco-Pasternak foundations are lower than those obtained from Winkler and Pasternak mediums, respectively. Furthermore, the critical blood velocity and frequency predicted by Pasternak medium is higher with respect to Winkler medium. It is perhaps due to the fact that the Winkler-type is capable to describe just normal load of the elastic medium while the Pasternak-type describes both transverse shear and normal loads of the elastic medium. However, the realistic and best medium for simulation of the surrounding tissue is visco-Pasternak foundation which considers the damping of the tissues around the arteries.
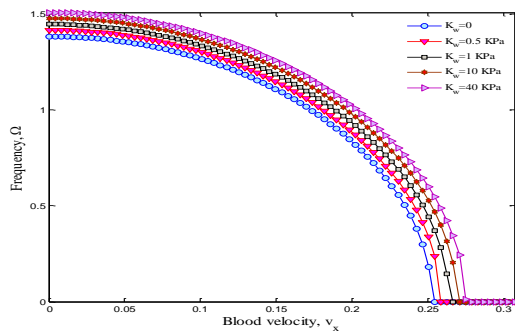

Fig.3
Frequency of arteries versus blood velocity for different spring constant of the tissues.
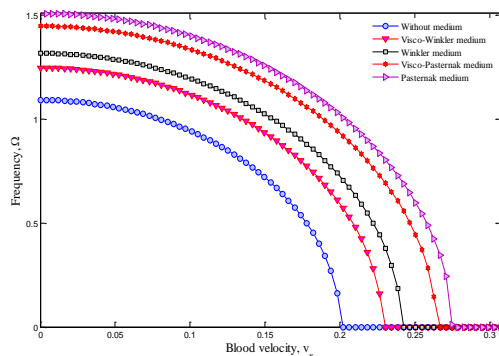

Fig.4
Frequency of arteries versus blood velocity for different tissues biomechanical models.

Figs. 5-7 illustrate the dimensionless transverse displacement of carotid artery versus length respectively, for different non-Newtonian models, spring constant of the elastic matrix and different surrounding elastic medium models. It is evident that the simply supported boundary conditions at both ends of carotid artery are satisfied. From Fig.5, it can be concluded that the dimensionless transverse displacement predicted by Newtonian model is lower than that of non-Newtonian models. Furthermore, the dimensionless transverse displacement of power law fluid is higher than that of Carreau and Casson models. Fig. 6 shows that with increasing the tissue stiffness, the transverse displacement of carotid artery decreases. It is due to that fact that with increasing elastic medium constant, the stiffness of artery increases. As can be seen from Fig. 7, considering elastic medium decreases the dimensionless transverse displacement of carotid artery. In addition, the dimensionless transverse displacement obtained from visco-Winkler and visco-Pasternak foundations are higher than those obtained from Winkler and Pasternak mediums, respectively.
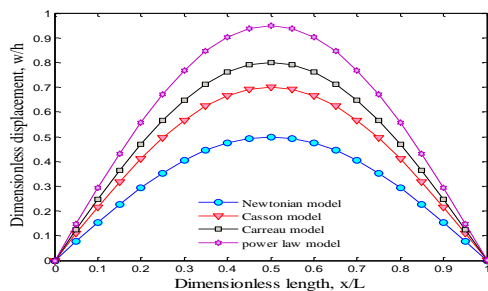
Fig.5
Transverse displacement of arteries versus length for Newtonian and non-Newtonian blood flow models.
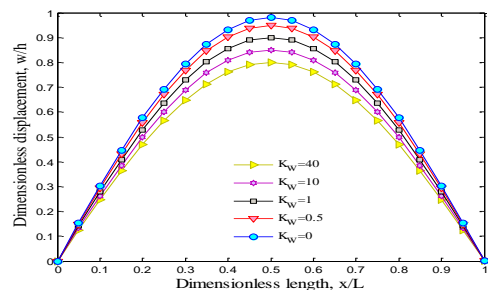
Fig.6
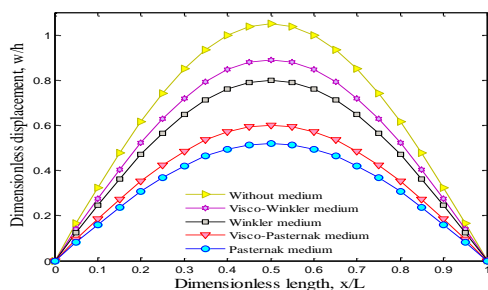Transverse displacement of arteries versus length for different spring constant of the tissues.

Fig.7
Transverse displacement of arteries versus length for different tissues biomechanical models.

4   CONCLUSIONS

In this study, a biomechanical model was presented for vibration and instability analysis of carotid arteries conveying blood surrounded by tissues. The blood flow was considered non-Newtonian based on Carreau, power law and Casson models. The tissues around the arteries were simulated by visc-Pasternak medium. Applying DQM, the frequency, critical blood velocity and transverse displacement of arteries were obtained. Results indicated that instability of the arteries will occur at higher blood velocities as the tissue becomes stronger and contiguous. In other words, contiguous tissue and muscles prevent from artery failure and tortuosity leads to wound recovery and improves the arteries and vein graft stability. In addition, the critical blood velocity predicted by Newtonian model is

higher than that of non-Newtonian models. Furthermore, the dimensionless transverse displacement predicted by Newtonian model is lower than that of non-Newtonian models. Meanwhile, the dimensionless transverse displacement obtained from visco-Winkler and visco-Pasternak foundations are higher than those obtained from Winkler and Pasternak mediums, respectively. Finally, it is hoped that the theoretical results presented in this paper would be helpful for experimental works by other researchers and development of new approaches for the treatment of arteries tortuosity and failure which has wide implications in vascular surgery, vascular physiology and pathology.

ACKNOWLEDGMENTS

REFERENCES

[1] Pancera P., Ribul M., Presciuttini B., Lechi A., 2000, Prevalence of carotid artery kinking in 590 consecutive subjects evaluated by Echocolordoppler. Is there a correlation with arterial hypertension, *Journal of Internal Medicine* **248**:7-12.

[2] Brown W.R., Moody D.M., Challa V.R., Thore C.R., Anstrom J.A., 2002, Venous collagenosis and arteriolar tortuosity in leukoaraiosis, *Journal of the Neurological Sciences* **203**:159-163.

[3] Hiroki M., Miyashita K., Oda M., 2002, Tortuosity of the white matter medullary arterioles is related to the severity of hypertension, *Cerebrovascular Disease* **13**:242-250.

[4] Aleksic M., Schutz G., Gerth S., Mulch J., 2004, Surgical approach to kinking and coiling of the internal carotid artery, *The Journal of Cardiovascular Surgery* **45**:43-48.

[5] Helisch A., Schaper W., 2003, Arteriogenesis: the development and growth of collateral arteries, *Microcirculation* **10**:83-97.

[6] Weibel J., Fields W.S., 1965, Tortuosity, coiling, and kinking of the internal carotid artery. Ii. relationship of morphological variation to cerebrovascular insufficiency, *Neurology* **15**:462-468.

[7] Jackson Z.S., Dajnowiec D., Gotlieb A.I., Langille B.L., 2005, Partial off-loading of longitudinal tension induces arterial tortuosity, *Arteriosclerosis, Thrombosis, and Vascular Biology* **25**:957-962.

[8] Han H.Ch., 2007, A biomechanical model of artery buckling, *Journal of Biomechanics* **40**:3672-3678.

[9] Han H.Ch., 2008, Nonlinear buckling of blood vessels: A theoretical study, *Journal of Biomechanics* **41**:2708-2713.

[10] Han H.Ch., 2009, Blood vessel buckling within soft surrounding tissue generates tortuosity, *Journal of Biomechanics* **42**:2797-2801.

[11] Han H.Ch., 2012, Mechanical buckling of artery under pulsatile pressure, *Journal of Biomechanics* **45**:1192-1198.

[12] Han H.Ch., 2013, Mechanical buckling of arterioles in collateral development, *Journal of Theoretical Biology* **316**:42-48.

[13] Pedley T.J., 1980, *The Fluid Mechanics of Large Blood Vessels*, Cambridge University Press, Cambridge.

[14] Cho Y.I., Kensey R., 1991, Effects of the non-newtonian viscosity of blood flows in a diseased arterial vessel. Part 1: steady flows, *Biorheology* **28**:241-262.

[15] Dash R.K., Jayaraman G., Metha K.N., 1999, Flow in a catheterized curved artery with stenosis, *Journal of Biomechanics* **32**:49-61.

[16] Chen J., Lu X.Y., 2004, Numerical investigation of the non-Newtonian blood flow in a bifurcation model with a non-planar branch, *Journal of Biomechanics* **37**:1899-1911.

[17] Barbara Johnston M., Johnston P.R., Corney S., Kilpatrick D., 2004, Non-Newtonian blood flow in human right coronary arteries: steady state simulations, *Journal of Biomechanics* **37**:709-720.

[18] Mandal P.K., 2005, An unsteady analysis of non-Newtonian blood flow through tapered arteries with a stenosis, *International Journal of Non-Linear Mechanics* **40**:151-164.

[19] Sankar D.S., Hemalatha K., 2007, A non-Newtonian fluid flow model for blood flow through a catheterized artery—Steady flow, *Applied Mathematical Modeling* **31**:1847-1864.

[20] Boyd J., Buick J.M., Green S., 2007, Analysis of the Casson and Carreau-Yasuda non-Newtonian blood models in steady and oscillatory flows using the lattice Boltzmann method, *Physics of Fluids* **19**:093103.

[21] Abdollahian M., Ghorbanpour Arani A., Mosallaie Barzoki A.A., Kolahchi R., Loghman A., 2013, Non-local wave propagation in embedded armchair TWBNNTs conveying viscous fluid using DQM, *Physica B* **418**:1-15.

[22] Ghorbanpour Arani A., Abdollahian M., Kolahchi R., Rahmati A.H., 2013, Electro-thermo-torsional buckling of an embedded armchair DWBNNT using nonlocal shear deformable shell model, *Composite Part B: Engineering* **51**:291-299.

[23] Taj M., Zhang J.Q., 2012, Analysis of vibrational behaviors of microtubules embedded within elastic medium by Pasternak model, *Biochemical and Biophysical Research Communications* **424**:89-93.

[24]   Ghorbanpour Arani A., Shiravand A., Rahi M., Kolahchi R., 2012, Nonlocal vibration of coupled DLGS systems embedded on Visco-Pasternak foundation, *Physica B* **407**:4123-4131.

[25]   Wang L., Ni Q., 2009, A reappraisal of the computational modelling of carbon nanotubes conveying viscous fluid, *Mechanics Research Communication* **36**:833-837.

[26]   Ghorbanpour Arani A., Kolahchi R., Khoddami Maraghi Z., 2013, Nonlinear vibration and instability of embedded double-walled boron nitride nanotubes based on nonlocal cylindrical shell theory, *Applied Mathematical Modeling* **37**:7685-7707.

[27]   Ghorbanpour Arani A., Kolahchi R., Mosallaie Barzoki A.A., Mozdianfard M.R., Noudeh Farahani S.M., 2012, Elastic foundation effect on nonlinear thermo-vibration of embedded double-layered orthotropic graphene sheets using differential quadrature method, *Journal of Mechanical Engineering Science* **227**:862-879.

[28]   Jozwik K., Obidowski D., 2010, Numerical simulations of the blood flow through vertebral arteries, *Journal of Biomechanics* **43**:177-185.

[29]   Cho Y.I., Kensey K.R., 1991, Effects of the non-Newtonian viscosity of blood on flows in a diseased arterial vessel. Part 1: steady flows, *Biorheology* **28**:241-262.

[30]   Han H.C., Zhao L., Huang M., Hou L.S., Huang Y.T., Kuang Z.B., 1998, Postsurgical changes of the opening angle of canine autogenous vein graft, *Journal of Biomechanical Engineering* **120**:211-216.